Fernando Viñals*, Flavia Correa, David Escribano, Lorena Hormazábal, Linder Diaz, Alberto Galindo, Belkys Zambrano, Gabriel Quiroz and Constanza Saint-Jean

Feasibility of extended ultrasound examination of the fetal brain between 24 and 37 weeks' gestation in low-risk pregnancies

https://doi.org/10.1515/jpm-2022-0605
Received December 14, 2022; accepted March 6, 2023;
published online April 18, 2023

Abstract

Objectives: To assess the feasibility of identifying fetal brain structures and anatomic landmarks included in the anterior complex (AC) and posterior complex (PC), as well as the proximal hemisphere (PH).
Methods: This was a prospective observational multicenter study of healthy pregnant women evaluated by ultrasound screening at 24 to 36 + 6 weeks' gestation. Six physicians performed transabdominal ultrasound, to obtain the planes required to visualize the AC, PC, and PH. Blind analysis by an expert and non-expert operator in fetal neurosonography was used to assess the structures included in each plane view.
Results: In the population studied (n=366), structure detection rates for AC were over 95 %, with an agreement of 96 % when comparing expert and non-expert examiners. Visualization of the corpus callosum crossing the midline was detected in over 97 and 96 % of cases for the AC and PC, respectively, with an agreement of over 96 %. The PH plane, particularly through the posterior access via the mastoid fontanelle, enabled visualization of the proximal anatomical structures in almost 95 % of cases. Detection of the corpus callosum through the AC and PC, both proximal/distal germinal matrix (AC) and proximal Sylvian fissure through the anterior access (PH) in the 24–25 + 6, 26–31 + 6 and 32–36 + 6 weeks' gestation groups were successful in over 96 % of cases with high level of agreement.
Conclusions: Inclusion of AC, PC, and PH later in pregnancy proves feasible with a high level of agreement between both expert and non-expert operators.

Keywords: anterior complex; central nervous system; posterior complex; prenatal diagnosis; proximal hemisphere.

Introduction

Although the screening evaluation of the fetal brain is focused around midgestation [1–4], there is a group of central nervous system (CNS) malformations whose phenotypic expression is not seen in earlier phases of the pregnancy, or the abnormality develops during the third trimester [5–7]. Since some of these findings are related to neurodevelopmental delay and could be associated with poor prognosis, it is necessary to prepare the expectant parents for the birth and plan the delivery timing and location to enhance postnatal investigations which could potentially improve postnatal outcome [7–9]. In exceptional cases, in countries where late termination of pregnancy is legal, the parents might be offered this option if a late CNS anomaly is detected [8, 9].

Third trimester anatomical evaluation of the CNS is not standardized and varies greatly according to the specific policies of each center and country. On the other hand, as pregnancy advances, visualization of the intracranial structures becomes more difficult due to advanced ossification of the calvarium.

Transabdominal sonography is the technique of choice for the screening examination of the fetal CNS in low-risk pregnancies [1–4]. We have recently reported that the inclusion of extended fetal brain examination into the routine 20–23 + 6 weeks' gestation ultrasound scan is feasible [10]. Such extended examination comprised the

***Corresponding author: Fernando Viñals**, Department of Obstetrics and Gynecology, Faculty of Medicine, University of Concepion, Sanatorio Aleman Clinic, Avenida Pedro de Valdivia 801, Concepcion, Chile, Phone: +56412794480, E-mail: fvinals@gmail.com. https://orcid.org/0000-0002-4272-8847
Flavia Correa, Fetal and Neonatal Ultrasonography Department, Hospital Lusíadas, Lisbon, Portugal
David Escribano and Alberto Galindo, Fetal Medicine Unit—Maternal and Child Health and Development Network, Department of Obstetrics and Gynaecology, University Hospital 12 de Octubre, 12 de Octubre Research Institute (imas12), Faculty of Medicine, Complutense University of Madrid, Madrid, Spain
Lorena Hormazábal, Linder Diaz, Belkys Zambrano, Gabriel Quiroz and Constanza Saint-Jean, Sanatorio Aleman Clinic and Department of Obstetrics and Gynaecology, Faculty of Medicine, University of Concepcion, Concepcion, Chile. https://orcid.org/0000-0001-9420-0406 (L. Diaz). https://orcid.org/0000-0002-4595-3652 (B. Zambrano)

assessment of anterior complex (AC) and posterior complex (PC), along with proximal hemisphere (PH) structures. These groups of structures could be considered important markers of fetal brain normality [11–13]. In this study, we sought to assess the performance of this same examination later in pregnancy.

Materials and methods

This was a prospective observational study performed on healthy women with singleton pregnancies and no increased risk of fetal CNS anomalies. All women provided written informed consent to participate in the study. Fetuses with chromosomal or structural anomalies, unknown pregnancy outcomes, or absence of informed consent were excluded. During the ultrasound scan, performed between 24 + 0 and 36 + 6 weeks' gestation, body mass index, fetal presentation, and gestational age (estimated by crown-rump length in the first trimester) were recorded. All participants were followed up to six months after birth and only those cases with normal development were included.

Five operators performed transabdominal (TA) ultrasound in Sanatorio Aleman Clinic, Concepcion, Chile using Voluson E6, E8, and E10 (GE Healthcare Ultrasound, Milwaukee, Wisconsin, USA) equipped with RAB 4–8 or 6D-MHZ probe. Another operator was located in University Hospital 12 de Octubre, Madrid, Spain. In that center, Toshiba Aplio MX SSA-780A (Tokyo, Japan) equipped with a 6-MHZ microconvex probe or Voluson E10 with 6D-MHZ probe were used for TA ultrasound. In total, 264 cases were collected from Chile and 102 cases from Spain.

Following a previous reported study [10], all sonologists were asked to store a five-second video clip of the following planes: transventricular plane (plane 1), transthalamic plane (plane 2) and transventricular plane (plane 3). In the transventricular plane, a magnified image of the anterior complex was stored (Figure 1) [11]. A fourth video clip was taken in the posterior complex (PC) plane (plane 4), that was obtained by slicing cranially from the transventricular plane until the interhemispheric fissure is interrupted by the crossing of the corpus callosum, in front of the parieto-occipital fissure (Figure 2). This axial section is parallel and immediately superior to the transventricular plane, and it is usually used to grade cortical development [11, 14, 15]. Lastly, the operator was instructed to return to the transthalamic plane and angle the transducer cranially by up to 45° [10, 12], which aims to assess the proximal hemisphere (PH) (plane 5). A slight modification was made to this maneuver, compared to previous reports [10], to adapt the ultrasound access to our mainly third trimester study population. Although ossification of the parietal bones progresses radially from the central primary focus toward the periphery of the bone and continues along all margins through fetal life [12], we expected a better ultrasound access at this gestational age by orienting the ultrasound beam to an anterior access PH visualization, via the sphenoidal fontanelle, and to a posterior access PH visualization, via the mastoid fontanelle (Figures 3 and 4). A five-second video clip of each proximal access was also stored, and examples of these are provided (Supplementary Material Video 1–5).

To evaluate whether the recognition of the structures included in each plane (Table 1) was influenced by the experience of the operator, we included a blind analysis by non-expert (L.H.) and expert (F.C.) in fetal neurosonography. Each structure was classified as seen or unseen. For statistical evaluation, we analyzed the results in the whole population of fetuses (24–36 + 6 weeks) as well as in the three following groups: 24–25 + 6, 26–31 + 6, and 32–36 + 6 weeks' gestation.

The primary outcome was defined as detection of the structures listed in Table 1 in the extended screening by both expert and non-expert examiner. The secondary outcome was to determine the agreement of visualizing these structures, between expert and non-expert examiner.

Data are presented as absolute numbers, percentages, means, medians (range interquartile and minimum-maximum range) and standard deviation and was performed with Excel 2022 (Microsoft 365 package. Microsoft Corp, Redmond, Washington) and SPSS (version 26, Statistical Package for Social Science, IBM Corp., Armonk, NY, USA). The Kolmogorov-Smirnov test was used to assess normal distribution. Chi-squared test and Fischer exact test were used to compare proportions and categorical variables. Confidence intervals of 95 % (95 % CI) were obtained according to the modified Wald method [16]. Percentage agreement and Cohen's kappa coefficient (κ) were calculated from 2×2 contingency tables and used to assess interobserver agreement between examiners A and B as well as intraobserver agreement for each examiner when comparing different planes [17]. $p \leq 0.05$ was considered statistically significant.

Results

Table 2 provides a summary of maternal and fetal ultrasound data from 366 patients studied. The visualization rates of the structures studied on the six planes by both examiners with different levels of experience are displayed in tables and Supplementary Tables (1–4).

Both examiners achieved high visualization rates for the structures included in the AC (Table 3) and PC (Supplementary Table 1), with significant agreement between expert and non-expert. Visualization of the corpus callosum crossing the midline was detected in over 97 and 96 % of cases in the AC and PC, respectively. In the case of the AC, both distal and proximal anterior horns of the lateral ventricle, subependymal germinal matrix and periventricular white matter presented at least 95 % visualization rates, with moderate to substantial level of agreement between both examiners. PH structures such as the posterior horn of the lateral ventricle, its atrium and choroid plexus and the posterior periventricular area were depicted less than 60 % of times in the transventricular plane (Supplementary Table 2). However, the PH plane, particularly through the posterior access via the mastoid fontanelle, enabled the visualization of the proximal anatomical structures in almost 95 % of the cases (Supplementary Table 3). Similarly, the anterior horn of the proximal lateral ventricle, its periventricular area and the proximal Sylvian fissure were visualized through the proximal anterior access via the sphenoidal fontanelle in more than 97 % of cases, with a moderate to almost perfect agreement between expert and

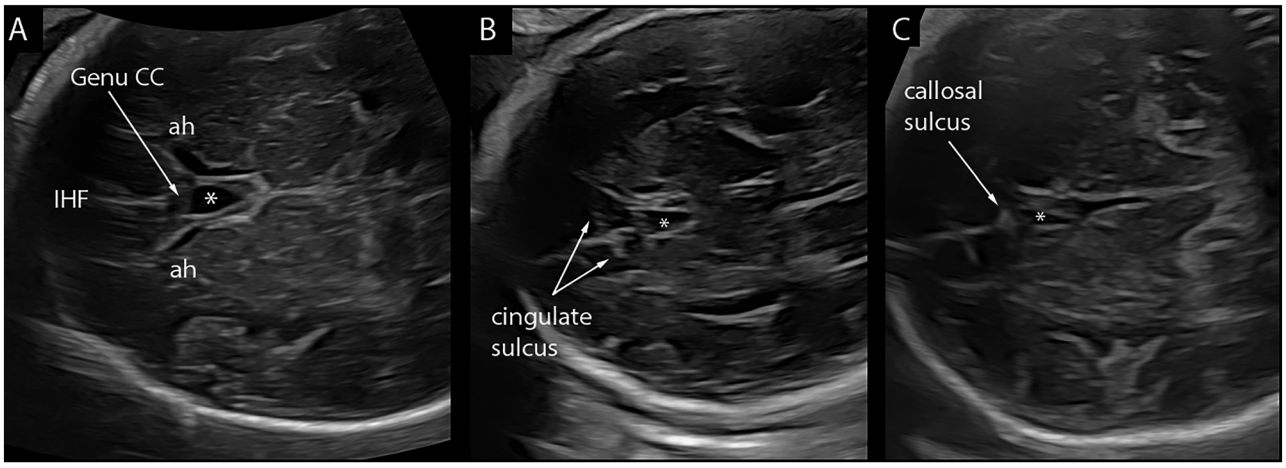

Figure 1: Anterior complex at 32 weeks' (A), 33 weeks' (B), and 34 (C) weeks' gestation. IHF, interhemispheric fissure; ah, anterior horn of the lateral ventricle; CC, corpus callosum; *, cavum septi pellucidi.

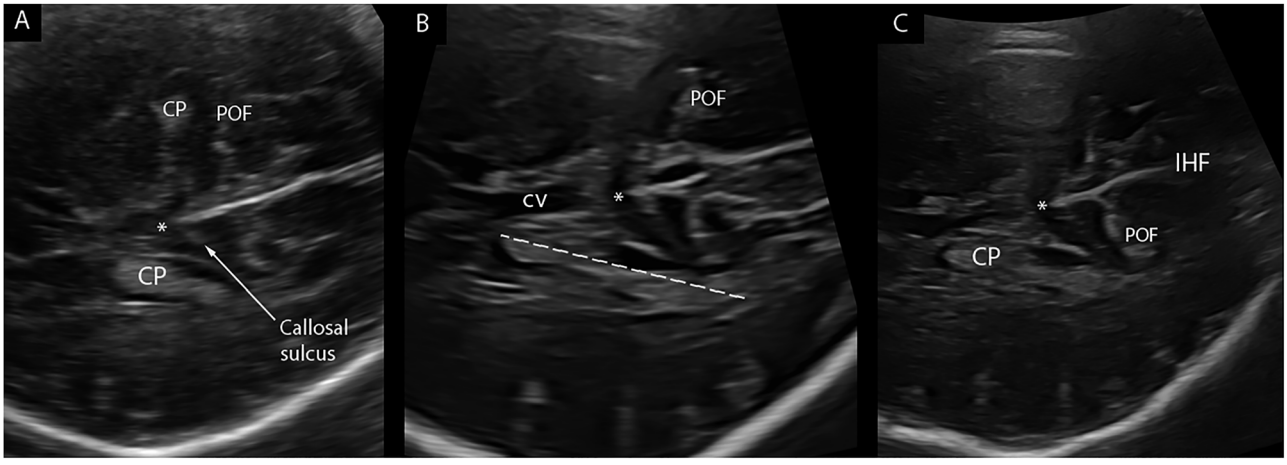

Figure 2: Posterior complex at 32 weeks' (A), 33 weeks' (B), and 34 (C) weeks'gestation. CP, choroid plexus of the lateral ventricle; cv, cavum vergae; POF, parieto-occipital fissure; IHF, interhemispheric fissure;*, corpus callosum. Dotted line corresponds to oblique disposition to the midline of the lateral ventricle and/or its choroid plexus.

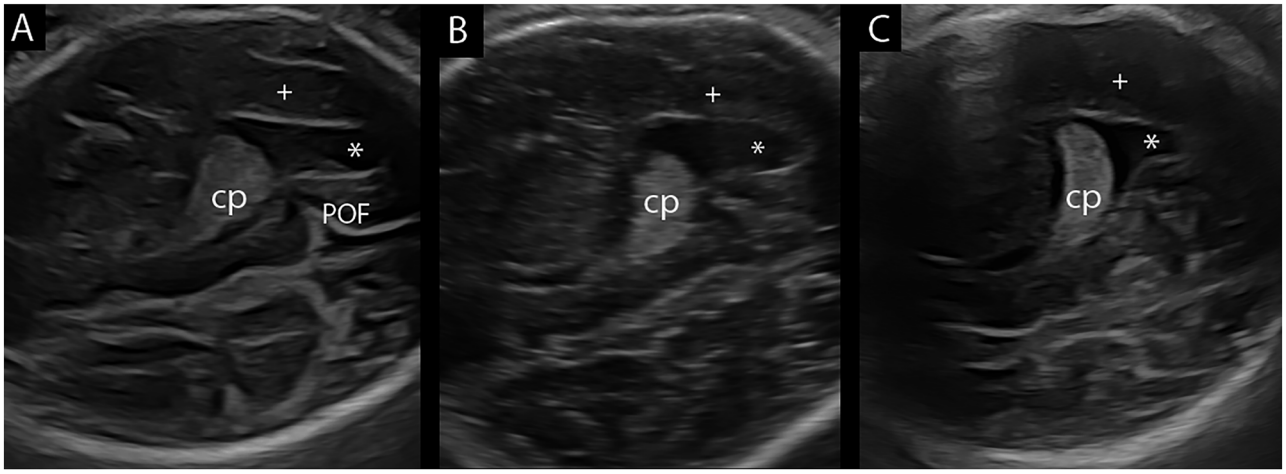

Figure 3: Posterior access of the proximal hemisphere at 32 weeks' (A), 33 weeks' (B), and 34 (C) weeks'gestation. cp, choroid plexus of the lateral ventricle; POF, parieto-occipital fissure; *, posterior horn of the proximal to the transducer lateral ventricle; +, periventricular white matter zone.

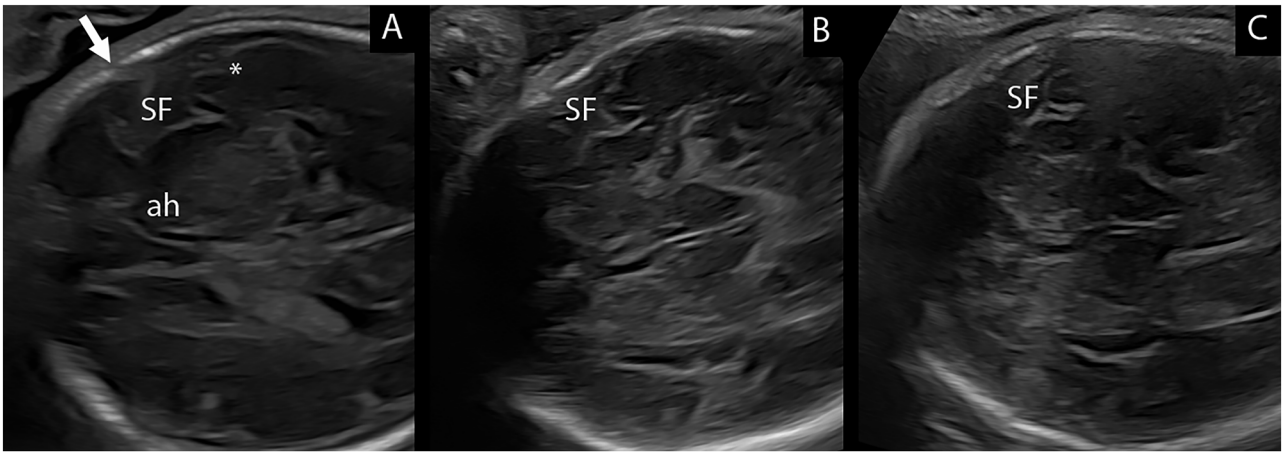

Figure 4: Anterior access of the proximal hemisphere at 32 weeks' (A), 33 weeks' (B), and 34 (C) weeks'gestation. ah, anterior horn of the proximal to the transducer lateral ventricle; SF, Sylvian fissure; *, superior temporal sulcus. Arrow corresponds to sphenoidal fontanel.

Table 1: Cerebral structures assessed in each plane.

Anterior complex
Interhemispheric fissure, callosal sulcus, genu of the corpus callosum, cavum septi pellucidi, anterior horns of the proximal and distal lateral ventricles, proximal and distal germinal matrix located in the external side of the lateral ventricles, white matter located in the external angle (lateral) of the proximal and distal frontal horns
Posterior complex
Corpus callosum, callosal sulcus, interhemispheric fissure, parieto-occipital fissure, oblique disposition to the midline of the proximal and distal lateral ventricles and/or both proximal and distal choroid plexus of the lateral ventricles
Transventricular plane
Structures included in the anterior complex are part of this plane. For both proximal and distal hemisphere: posterior horn of the lateral ventricles with wall integrity, contour, and uniformly anechoic fluid content, atrium, choroid plexus fills the ventricular cavity and is closely apposed to both the medial and lateral walls of the ventricle, and periventricular white matter zone is smooth and regular in its echogenicity. Furthermore, cortical surface of both distal and proximal temporal and occipital lobes.
Proximal hemisphere
Anterior access (sphenoidal fontanelle and sutures that converge to it): visualization of the anterior horn of the lateral ventricle with smooth inner surface and uniformly anechoic fluid content. Periventricular white matter zone is smooth and regular in its echogenicity. Cortical surface of the frontal lobe. The Sylvian fissure is visible, and its shape is comparable with that of the distal hemisphere.
Posterior access (mastoid fontanelle and sutures that converge to it): Atrium and posterior horn of the proximal lateral ventricle with wall integrity, contour, and uniformly anechoic fluid content. Periventricular white matter zone is smooth and regular in its echogenicity. Cortical surface of the temporal and occipital lobes

non-expert examiners (Supplementary Table 4). In the group of 32–36 + 6 weeks' of gestation the detection of the corpus callosum at the level of the anterior and posterior complex was higher than 95 % for both examiners and the visualization of the proximal and distal germinal matrix at the level of the AC exceeded 96 % as well. Similar rates of detection were achieved for the periventricular white matter at the level of the posterior horn of the proximal lateral ventricle and the proximal Sylvian fissure, both through proximal hemisphere access. Identification of these structures reach high level of agreement between the two examiners (Table 4).

The kappa values corresponding to the anterior complex and proximal hemisphere were rated as moderate to good (between 0.4 and 0.8) or very good (between 0.8 and 1), in most cases. Regarding the posterior complex, kappa values were low to moderate, despite a very high percent agreement. This could be explained by the fact that in the posterior complex the percent agreement tends to be close to 95 %, unlike in the anterior complex where agreement is close to 100 %. These differences, which are small according to the percentage of agreement, have a greater impact in the kappa values (Table 3 and Supplementary Tables 1–4).

Table 2: Maternal and ultrasound data in 366 women with singleton pregnancy between 24-36 + 6 weeks' gestation.

Parameter			Value
Maternal (BMI, kg/m^2)			median 26.4 (range 16.1–45.2) (IQR: 23.4–28.7) (max-min: 16.1–45.2)
Ultrasound (GA, weeks')	24-36 + 6	(n=366)	median 29 + 2 (IQR: 24+6d-34+4d) (max-min: 24–36+6d)
	24-25 + 6		137 (37.4 %)
	26-31 + 6		79 (21.6 %)
	32-36 + 6		150 (41 %)
Fetal presentation (n=366)	Cephalic		296 (80.9 %)
	Breech		61 (16.6 %)
	Transverse		9 (2.5 %)

BMI, body mass index; GA, gestational age.

Discussion

This prospective study combines the assessment of AC, PC, and PH in normal fetuses mainly in the third trimester by operators with varying levels of experience, analyzing diverse populations of low-risk pregnant women with different ultrasound equipments. Our results indicate that both non-expert and expert operators can identify the structures included in AC, PC and PH in more than 95 % of cases. As is the case between 20-23 + 6 weeks' gestation [10], AC and PC complex visualization, as well as real-time access to the PH, also proved to be feasible later in pregnancy. Moreover, some important structures of the mentioned planes, when stratified by gestational age, can be excellently depicted even at 36 weeks gestation.

In the last decade we have witnessed the inclusion of the outflow tracts view to the cardiac screening examination of low-risk fetuses to maximize the detection of heart anomalies during the midtrimester scan. At that time, it became clear that optimization of anatomical targets screened prenatally offered better potential to ultrasound diagnosis [18]. In our work, the focus of study should be four groups of cerebral anatomical landmarks, obtained from transabdominal axial planes [10–13]. The first corresponds to the AC, assessing targets aimed to analyze cortical development (interhemispheric fissure, callosal sulcus and the aspect of the anterior horn of the lateral ventricles), midline structures (genu of the corpus callosum and cavum septi pellucidi), proximal and distal germinal matrix located in the external side of the lateral ventricles and the white matter located in the external angle (lateral) of the proximal and distal frontal horns. The second corresponds to the PC, which also incorporates structures aimed to evaluate cortical development (interhemispheric fissure, callosal sulcus and parietooccipital fissure), as well as direct visualization of the posterior component of the

Table 3: Anterior complex: detection of structures, percentage of agreement, and kappa index.

Anterior complex	Percentage of detection examiner A 24 + 0 to 36 + 6	(Detected/ total)	Percentage of detection examiner B 24 + 0 to 36 + 6	(Detected /total)	Percentage of agreement 24 + 0 to 36 + 6	(95 % CI)	Kappa	(95 % CI)	p
IHF	99.7	(365/366)	99.5	(364/366)	99.7	(98.3–99.9)	0.66	(0.57–0.76)	0.0001
Callosal sulcus	96.7	(354/366)	98.6	(361/366)	97.5	(95.3–98.7)	0.46	(0.36–0.55)	0.0001
Genu of CC	97.3	(356/366)	98.9	(362/366)	97.8	(95.6–98.9)	0.42	(0.32–0.51)	0.0001
CSP	100	(366/366)	100	(366/366)	100	(98.7–100)	NA	NA	NA
Proximal anterior horn LV	99.1	(363/366)	98.4	(360/366)	98.6	(96.7–99.5)	0.43	(0.34–0.53)	0.0001
Distal anterior horn LV	98.1	(359/366)	97.3	(356/366)	97.5	(95.3–98.7)	0.45	(0.35–0.55)	0.0001
Proximal subependymal germinal matrix	99.5	(364/366)	98.4	(360/366)	98.9	(97.1–99.6)	0.49	(0.4–0.58)	0.0001
Distal subependymal germinal matrix	98.6	(361/366)	98.1	(359/366)	99.4	(97.9–99.9)	0.83	(0.72–0.93)	0.0001
Proximal anterior periventricular white matter	95.1	(348/366)	95.9	(351/366)	96.4	(93.9–97.9)	0.58	(0.48–0.68)	0.0001
Distal anterior periventricular white matter	97.3	(356/366)	95.6	(350/366)	97.2	(94.9–98.5)	0.6	(0.5–0.7)	0.0001

p calculated with Chi-squared test or Fischer exact test. IFH, interhemispheric fissure; CC, corpus callosum; CSP, cavum septi pellucidi; PO, parietooccipital; NA, not available; LV, lateral ventricle.

Table 4: Genu of the corpus callosum (anterior complex), corpus callosum (posterior complex), proximal and distal geminal matrix (anterior complex), proximal Sylvian fissure and posterior horn and periventricular white matter of the proximal lateral ventricle (proximal hemisphere): detection, percentage of agreement and kappa index at different gestational ages.

	Percentage of detection examiner A 24 + 0 to 25 + 6 (detected/total)	Percentage of detection examiner B 24 + 0 to 25 + 6 (detected/total)	Percentage of greement 24 + 0 to 25 + 6 (95 % CI)	Kappa (95 % CI)	Percentage of detection examiner A 26 + 0 to 31 + 6 (detected/total)	Percentage of detection examiner B 26 + 0 to 31 + 6 (detected/total)	Percentage of agreement 26 + 0 to 31 + 6 (95 % CI)	Kappa (95 % CI)	Percentage of detection examiner A 32 + 0 to 36 + 6 (detected/total)	Percentage of detection examiner B 32 + 0 to 36 + 6 (detected/total)	Percentage of agreement 32 + 0 to 36 + 6 (95 % CI)	Kappa (95 % CI)	p
Genu of CC (anterior complex)	100 (137/137)	100 (137/137)	100 (96.7–100)	NA NA	98.7 (78/79)	100 (79/79)	98.7 (92.5–99.9)	0 (0-0)	94 (141/150)	97.3 (146/150)	95.3 (90.5–97.9)	0.44 (0.29–0.58)	0.0001
Proximal subependymal germinal matrix (anterior complex)	100 (137/137)	100 (137/137)	100 (96.7–100)	NA NA	100 (79/79)	100 (79/79)	100 (94.4–100)	NA NA	98.7 (148/150)	96 (144/150)	97.3 (93.1–99.2)	0.49 (0.35–0.62)	0.0001
Distal subependymal germinal matrix (anterior complex)	100 (137/137)	100 (137/137)	100 (96.7–100)	NA NA	98.7 (78/79)	98.7 (78/79)	100 (94.4–100)	1 (0.78–1)	97.3 (146/150)	96 (144/150)	98.6 (94.9–99.9)	0.79 (0.63–0.95)	0.0001
CC (posterior complex)	94.2 (129/137)	99.2 (136/137)	94.9 (89.6–97.7)	0.21 (0.11–0.31)	96.2 (76/79)	97.5 (77/79)	96.2 (88.9–99.1)	0.38 (0.16–0.6)	98 (147/150)	98.7 (148/150)	98 (94–99.5)	0.39 (0.23–0.54)	0.0001
Posterior horn of LV (proximal cerebral hemisphere -posterior access-)	99.2 (136/137)	100 (137/137)	99.2 (95.5–99.9)	0 (0-0)	98.7 (78/79)	100 (79/79)	98.7 (92.5–99.9)	0 (0-0)	98.7 (148/150)	85.3 (128/150)	86.6 (80.2–91.2)	0.15 (0.06–0.22)	0.001
Periventricular white matter (proximal cerebral hemisphere -posterior access-)	96.4 (132/137)	100 (137/137)	96.4 (91.5–98.6)	0 (0-0)	100 (79/79)	100 (79/79)	100 (94.4–100)	NA NA	96.7 (145/150)	96 (144/150)	98 (94–99.5)	0.71 (0.29–0.58)	0.0001
Sylvian fissure (proximal cerebral hemisphere -anterior access-)	97.8 (134/137)	99.2 (136/137)	98.5 (94.5–99.9)	0.49 (0.35–0.63)	98.7 (78/79)	98.7 (78/79)	100 (94.4–100)	1 (0.78–1)	97.3 (146/150)	96.6 (145/150)	96.6 (92.2–98.7)	0.42 (0.26–0.58)	0.0001

p calculated with Chi-squared test or Fischer exact test. CC, corpus callosum; LV, lateral ventricle.

corpus callosum crossing the midline (depending on the gestational age, body or splenium) and an oblique disposition to the midline of the proximal and distal lateral ventricles and/or both proximal and distal choroid plexus of the lateral ventricles. The other two planes correspond to the anterior and posterior access of the proximal hemisphere. The first uses the sphenoid fontanel as acoustic window and mainly enables analysis of the proximal Sylvian fissure and the periventricular white matter. Finally, the posterior access through the mastoid fontanel serves to evaluate the atrium and posterior horn of the proximal lateral ventricle, its wall integrity, contour, and uniformly anechoic fluid content. In addition, this view can confirm that the periventricular white matter zone is smooth and regular in its echogenicity.

Lastly, it is well known that in the standard transventricular plane, usually only the distal hemisphere to the transducer is clearly visualized since bony attenuation precludes good access to the PH [1]. However, visualization and comparison of both hemispheres, particularly both distal and proximal lateral ventricles, periventricular white matter and Sylvian fissure, ensures a more robust and integral qualitative evaluation of the fetal brain (Supplementary Figure 1) [12]. Furthermore, daily practice recognizes the usefulness of comparison between paired anatomical structures that usually facilitates their subjective interpretation when only one of them is affected by anomalies [19]. This may be relevant in the case of patterns of sulcation, which evolve rapidly through gestation [20, 21], meaning many of the gyration anomalies can only be suspected in later stages of the pregnancy and can affect one or both hemispheres [22, 23]. Similarly, it is also necessary to consider that other abnormal conditions such as hypoxic-ischemic lesions, hemorrhages, schizencephaly, ventriculomegaly and tumors, that may have an important impact in neurodevelopmental outcome, can affect only one hemisphere [12]. Therefore, it is important to enhance the anatomical assessment of the whole fetal brain, even in low-risk pregnancies, and this can be achieved following our proposal, which facilitates PH examination simply by angling the transducer from the standard transthalamic plane. Finally, although we did not aim to establish which is the best gestational age for this late fetal brain assessment, from a clinical point of view it is of note that the rates of visualization of the structures included in the different planes as well the level of agreement between operators remained constant in the different gestational age windows, including around 36 weeks, where it is currently being recommended to perform the routine third trimester scan [24].

The main strengths of this study are: its prospective and multicenter nature, the wide range of gestational ages; and the use of very precise definitions of anatomical landmarks and the respective standardized planes. The main limitation of the study is that further prospective research is needed to confirm its usefulness for improving fetal brain anomalies detection.

Our proposal improves operator understanding of what could be achieved and depicted using well defined anatomical landmarks included in transabdominal axial sections. Inclusion of AC, PC, and PH later in pregnancy proves feasible with a high level of agreement between both expert and non-expert operators. Our results could help to standardize fetal CNS anatomical evaluation in the second half of pregnancy, to improve the suspicion and detection of subtle and unilateral cerebral anomalies which may develop late in pregnancy.

Research funding: None declared.
Author contributions: All authors have accepted responsibility for the entire content of this manuscript and approved its submission.
Competing interests: Authors state no conflict of interest.
Informed consent: Informed consent was obtained from all individuals included in this study.
Ethical approval: The local Institutional Review Board deemed the study exempt from review.

References

1. Malinger G, Paladini D, Haratz KK, Monteagudo A, Pilu GL, Timor-Tritsch IE. ISUOG practice guidelines (updated): sonographic examination of the fetal central nervous system. Part 1: performance of screening examination and indications for targeted neurosonography. Ultrasound Obstet Gynecol 2020;56:476–84.
2. AIUM practice Parameter for the performance of detailed second- and third-trimester diagnostic obstetric ultrasound examinations. J Ultrasound Med 2019;38:3093–100.
3. De Robertis V, Sen C, Timor-Tritsch I, Chaoui R, Volpe P, Galindo A, et al. WAPM-world association of Perinatal medicine practice guidelines: fetal central nervous system examination. J Perinat Med 2021;49: 1033–41.
4. Salomon L, Alfirevic Z, Berghella V, Bilardo CM, Chalouhi GE, Da Silva Costa F, et al. ISUOG Practice Guidelines (updated): performance of the routine mid-trimester fetal ultrasound scan. Ultrasound Obstet Gynecol 2022;59:840–56.
5. Malinger G, Lerman-Sagie T, Watemberg N, Rotmensch S, Lev D, Glezerman M. A normal second-trimester ultrasound does not exclude intracranial structural pathology. Ultrasound Obstet Gynecol 2002;20: 51–6.
6. Yinon Y, Katorza E, Nassie DI, Ben-Meir E, Gindes L, Hoffmann C, et al. Late diagnosis of fetal central nervous system anomalies following a normal second trimester anatomy scan. Prenat Diagn 2013;33:929–34.

7. Ficara A, Syngelaki A, Hammami A, Akolekar R, Nicolaides KH. Value of routine ultrasound examination at 35-37 weeks' gestation in diagnosis of fetal abnormalities. Ultrasound Obstet Gynecol 2020;55:75–80.
8. Bakalis S, Cao K, Johal N, Cuckow P, Pandya P. The value of the routine third trimester ultrasound scan in antenatal care Problems with guidance and outdated data in a highly technological field. Eur J Obstet Gynecol 2020;245:51–5.
9. Manegold G, Tercanli S, Struben H, Huang D, Kang A. Is a routine ultrasound in the third trimester justified? Additional fetal anomalies diagnosed after two previous unremarkable ultrasound examinations. Ultraschall Med 2011;32:381–6.
10. Hormazabal L, Correa F, Escribano D, Quiroz G, Saint-Jean C, Espinel A, et al. Feasibility and agreement of including anterior-posterior complexes and landmarks of the proximal hemisphere into basic examination of the fetal brain: a prospective study. Prenat Diagn 2020; 40:596–604.
11. Viñals F, Correa F, Gonçalves-Pereira PM. Anterior and posterior complexes: a step towards improving neurosonographic screening of midline and cortical anomalies. Ultrasound Obstet Gynecol 2015;46: 585–94.
12. Viñals F, Correa F. Proximal cerebral hemisphere: should we continue to assume symmetry or is it time to look at it routinely? Fetal Diagn Ther 2016;40:79–80.
13. Viñals F, Correa F, Tubau A, Alonso I, Serra V, Herraiz I, et al. New insights into the anterior complex. Fetal Diagn Ther 2020;47:514–8.
14. Pistorius LR, Stoutenbeek P, Groenendaal F, de Vries L, Manten G, Mulder E, et al. Grade and symmetry of normal fetal cortical development: a longitudinal two- and three-dimensional ultrasound study. Ultrasound Obstet Gynecol 2010;36:700–8.
15. Alonso I, Borenstein M, Grant G, Narbona I, Azumendi G. Depth of brain fissures in normal fetuses by prenatal ultrasound between 19 and 30 weeks of gestation. Ultrasound Obstet Gynecol 2010;36:693–9.
16. Agresti A, Coull B. Approximate is better than "exact" for interval estimation of binomial proportions. Am Statistician 1998;52: 119–26.
17. Brennan P, Silman A. Statistical methods for assessing observer variability in clinical measures. BMJ 1992;304:1491–4.
18. Carvalho JS, Allan LD, Chaoui R, Copel JA, DeVore GR, Hecher K, et al. ISUOG Practice Guidelines (updated): sonographic screening examination of the fetal heart. Ultrasound Obstet Gynecol 2013;41: 348–59.
19. Labadini C, Macé P, Quarello E. Examination of Sylvian fissure can and should be performed bilaterally during screening: let's not leave it to chance. Ultrasound Obstet Gynecol 2022;60:698–700.
20. Griffiths PD, Reeves M, Morris J, Larroche JC. Atlas of Fetal and Postnatal Brain MR. Philadelphia: Saunders Elsevier; 2010:7 p.
21. Garel C. MRI of the Fetal Brain. Normal Development and Cerebral Pathologies. Heidelberg: Springer-Verlag; 2004:13 p.
22. Quarello E, Guibaud L. Prenatal sonographic assessment of Sylvian fissure operculization (SFO): importance of distinguishing between screening and diagnostic tools and selecting precise anatomical landmarks. Ultrasound Obstet Gynecol 2020;56:786–8.
23. Pooh RK, Machida M, Nakamura T, Uenishi K, Chiyo H, Itoh K, et al. Increased Sylvian fissure angle as early sonographic sign of malformation of cortical development. Ultrasound Obstet Gynecol 2019;54:199–206.
24. Roma E, Arnau A, Berdala R, Bergos C, Montesinos J, Figueras F. Ultrasound screening for fetal growth restriction at 36 vs 32 weeks' gestation: a randomized trial (ROUTE). Ultrasound Obstet Gynecol 2015;46:391–7.

Supplementary Material: The online version of this article offers supplementary material (https://doi.org/10.1515/jpm-2022-0605).